Electronic Supplementary Material (ESI) for Green Chemistry.

Supporting Information

Defect Engineering of Nickel Hydroxide Nanosheets by Ostwald Ripening for Enhanced Selective Electrocatalytic Alcohol Oxidation

Xianlang Chen, Xing Zhong, Bowen Yuan, Suiqin Li, Yongbing Gu, Qiaoqiao Zhang, Guilin Zhuang, Xiaonian Li, Shengwei Deng and Jian-guo Wang**

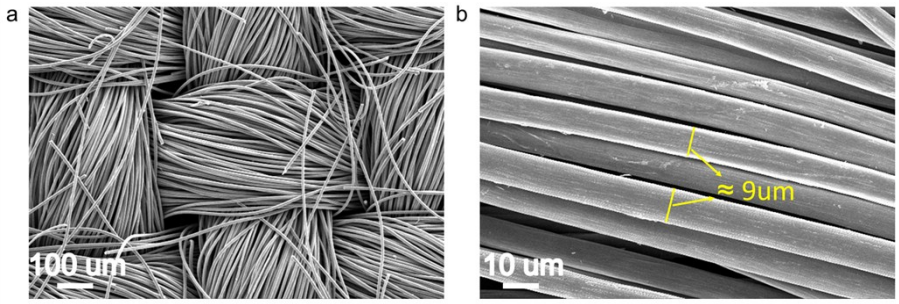

Figure S1. SEM images of CF.

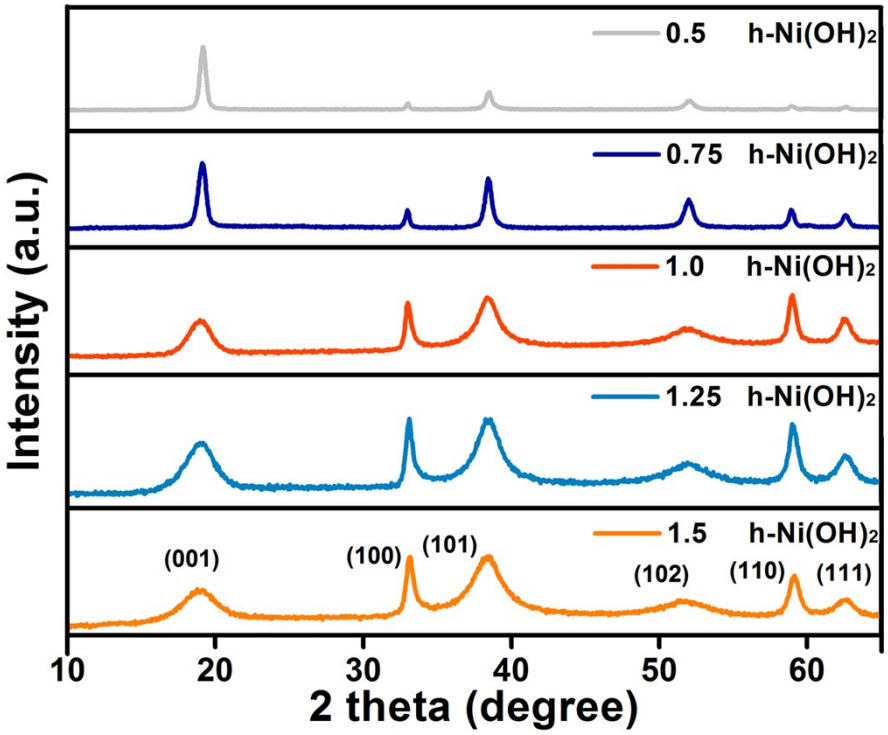

Figure S2. XRD patterns of 0.5, 0.75, 1.0, 1.25 and 1.5 h-Ni(OH)$_2$.

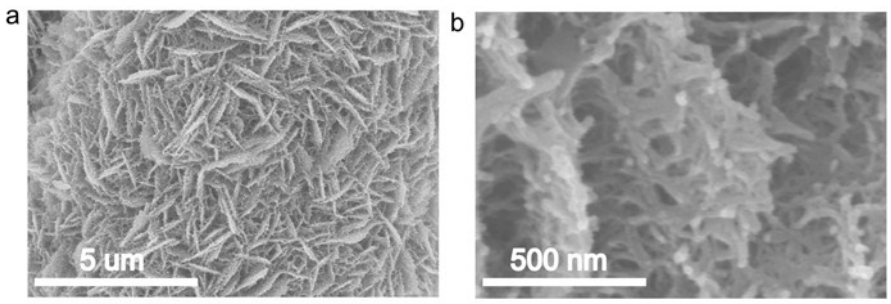

Figure S3. SEM images of 1.0 NiZn(OH)$_2$.

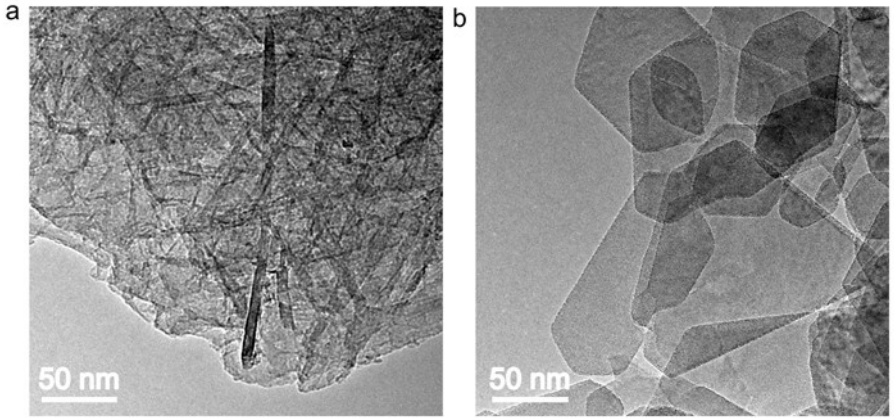

Figure S4. TEM images of (a) 1.0 $NiZn(OH)_2$, (b) 1.0 h-Ni $(OH)_2$.

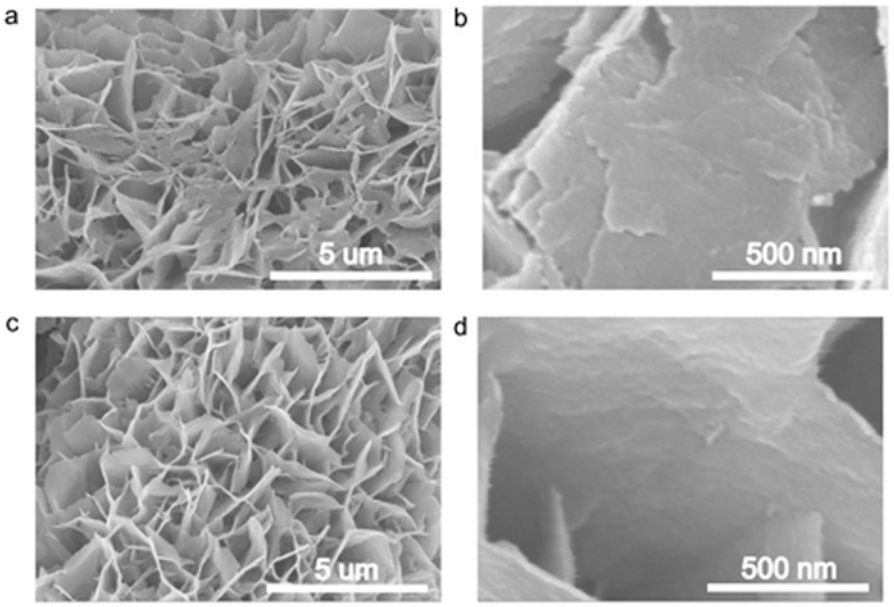

Figure S5. SEM images of (a, b) 0.5 $NiZn(OH)_2$, (c, d) 0.5 h-Ni $(OH)_2$.

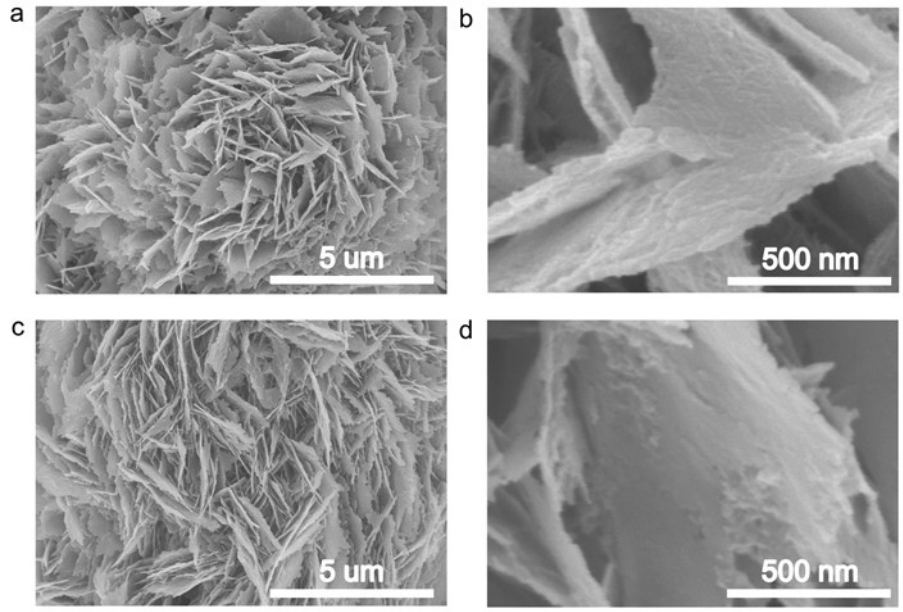

Figure S6. SEM images of (a, b) 0.75 $NiZn(OH)_2$, (c, d) 0.75 h-Ni $(OH)_2$.

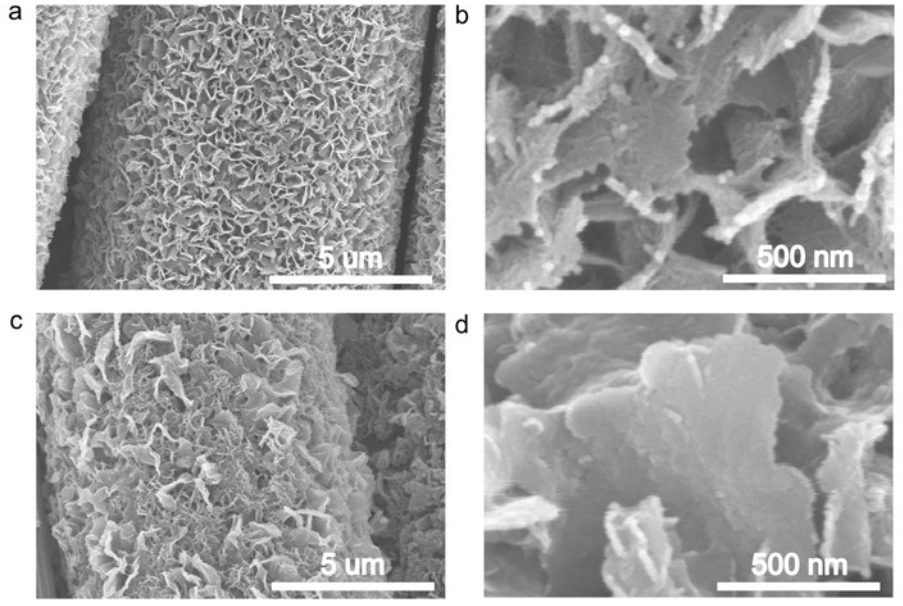

Figure S7. SEM images of (a, b) 1.25 $NiZn(OH)_2$, (c, d) 1.25 h-Ni $(OH)_2$.

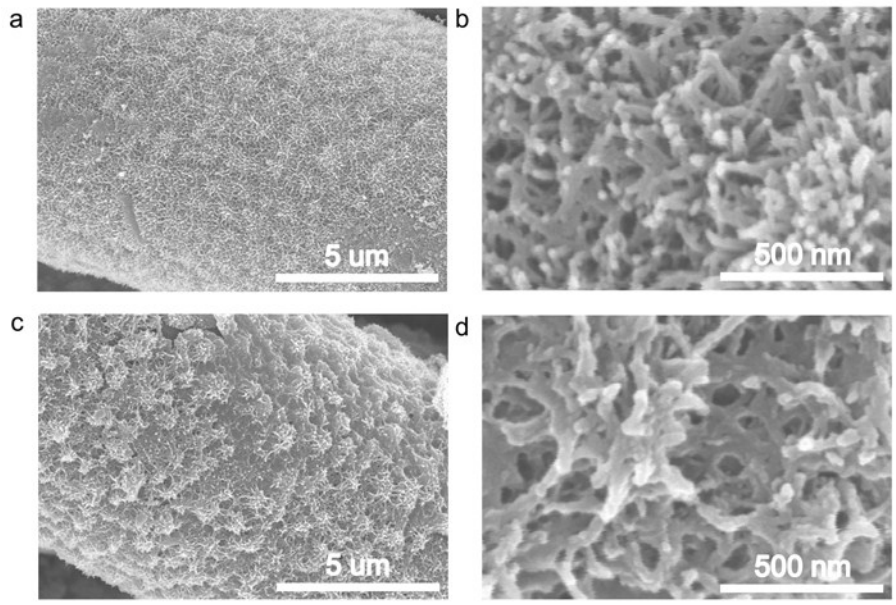

Figure S8. SEM images of (a, b) 1.5 $NiZn(OH)_2$, (c, d) 1. 5 h-$Ni(OH)_2$.

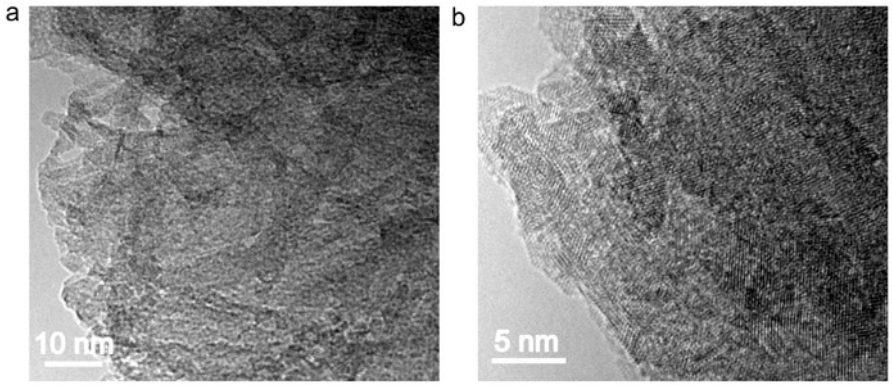

Figure S9. TEM images of (a, b) 1.0 $NiZn(OH)_2$.

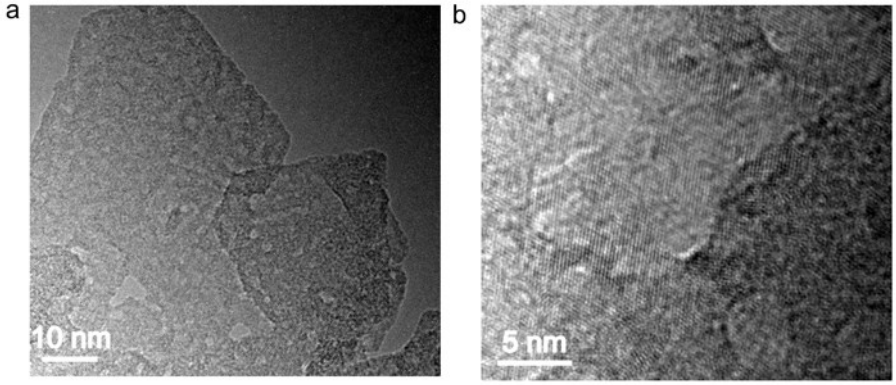

Figure S10. TEM images of (a, b) 0.5 h-$Ni(OH)_2$.

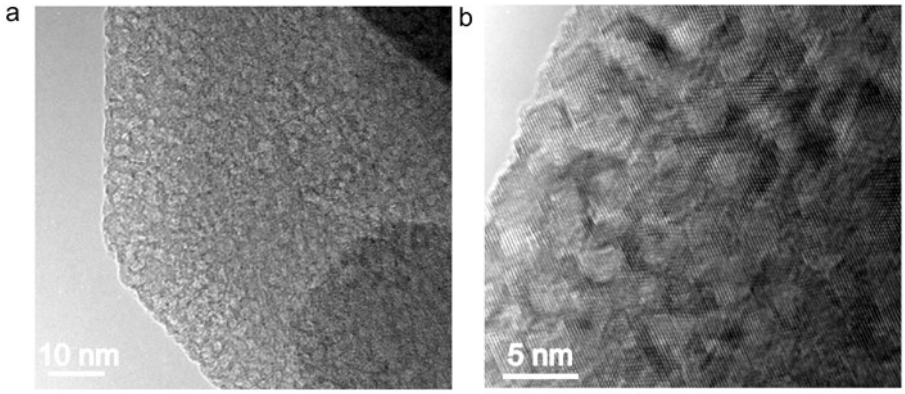

Figure S11. TEM images of (a, b) 0.75 h-$Ni(OH)_2$.

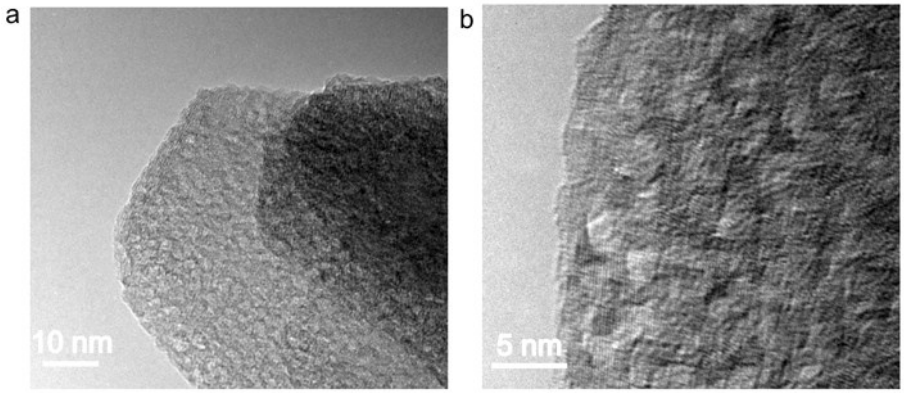

Figure S12. TEM images of (a, b) 1.25 h-$Ni(OH)_2$.

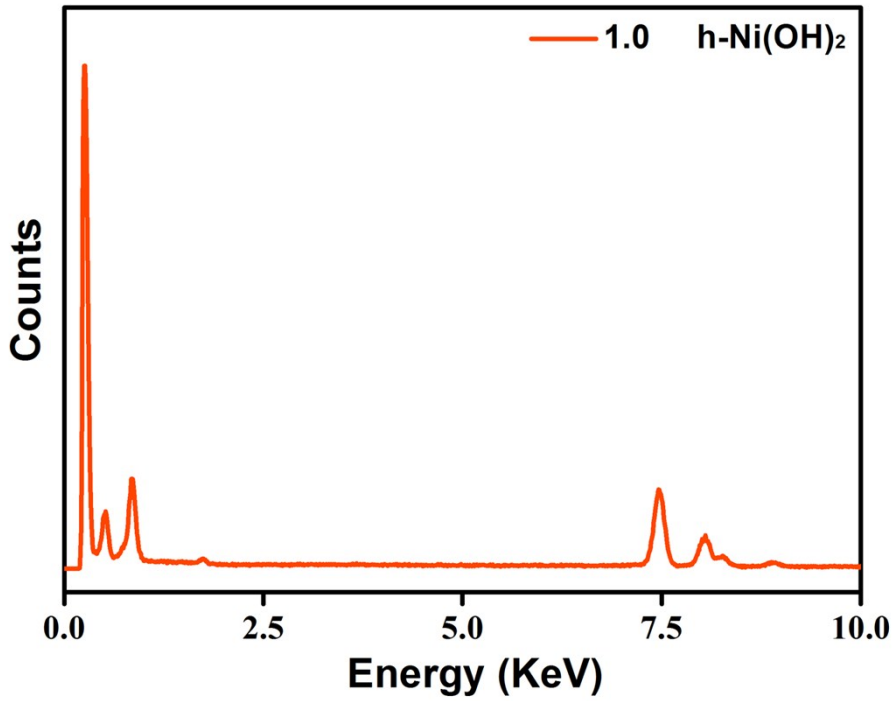

Figure S13. EDX spectrum of 1.0 h-Ni(OH)$_2$.

Table S1. The relative ratio of different kinds of oxygen in as-synthesized h-Ni(OH)$_2$.

Samples	surface O-C=O /%	Adsorbed OH /%	Lattice OH /%	Lattice O /%
0.5 h-Ni(OH)$_2$	8.26	22.03	61.10	6.61
0.75 h-Ni(OH)$_2$	6.48	31.76	52.35	9.41
1.0 h-Ni(OH)$_2$	9.88	34.03	47.20	8.89
1.25 h-Ni(OH)$_2$	10.08	31.53	50.82	7.57
1.5 h-Ni(OH)$_2$	8.57	15.91	68.79	6.73

Table S2. BET specific surface area of various materials.

Material	BET Surface Area /m^2g^{-1}
0.5 h-$Ni(OH)_2$	31.01
0.75 h-$Ni(OH)_2$	37.94
1.0 h-$Ni(OH)_2$	63.89
1.25 h-$Ni(OH)_2$	88.92
1.5 h-$Ni(OH)_2$	108.19

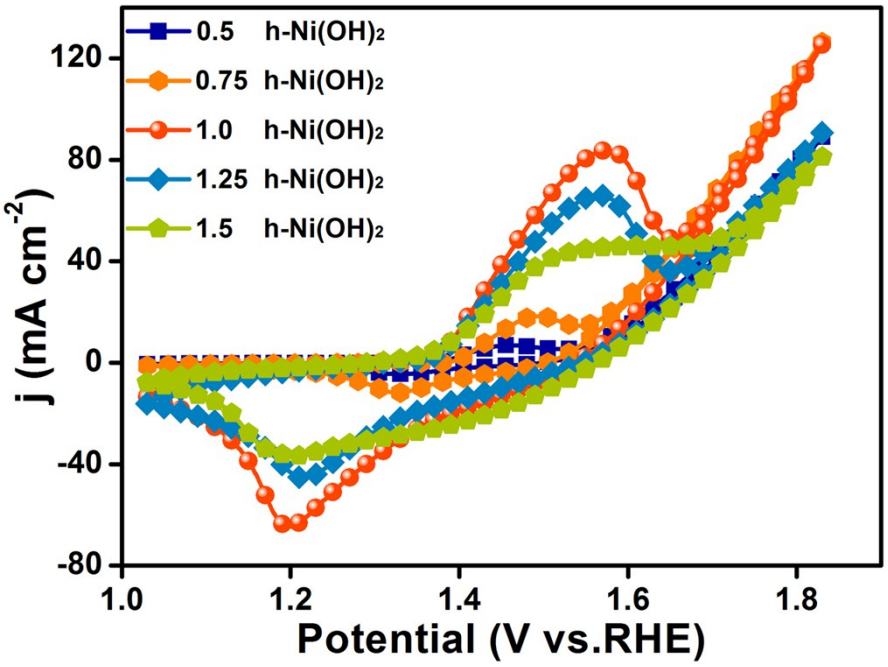

Figure S14. The CV curves of 0.5, 0.75, 1.0, 1.25 and 1.5 h-$Ni(OH)_2$.

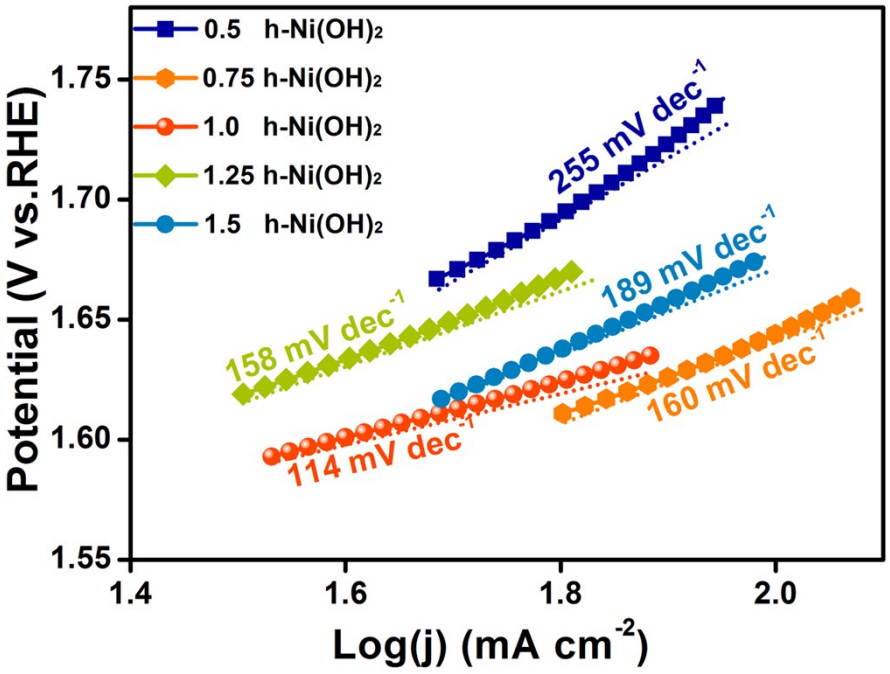

Figure S15. Tafel plots derived from LSV curves of 0.5, 0.75, 1.0, 1.25 and 1.5 h-$Ni(OH)_2$.

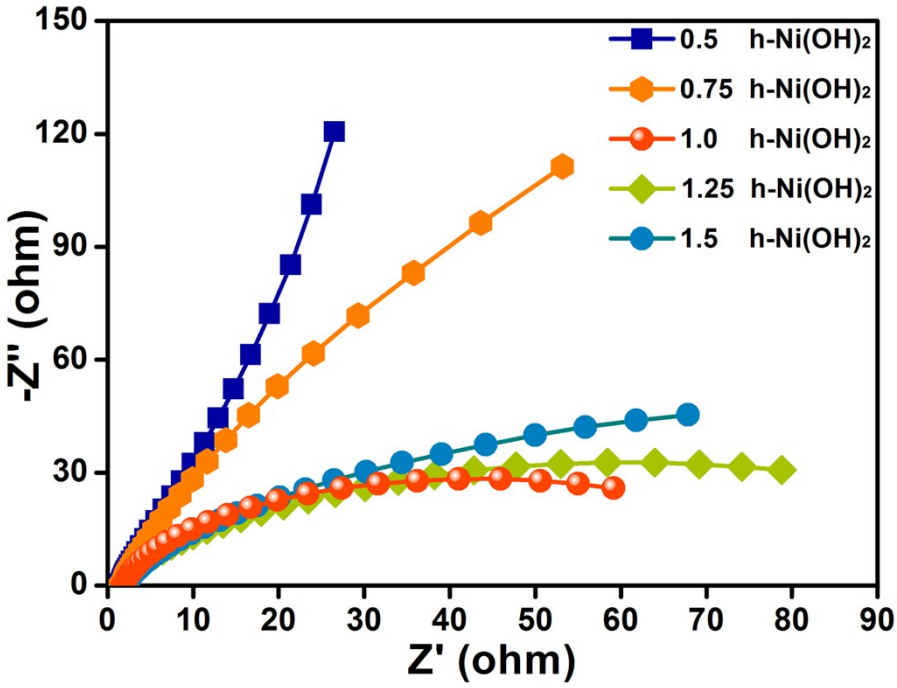

Figure S16. Electrochemical impedance spectra of 0.5, 0.75, 1.0, 1.25 and 1.5 h-$Ni(OH)_2$.

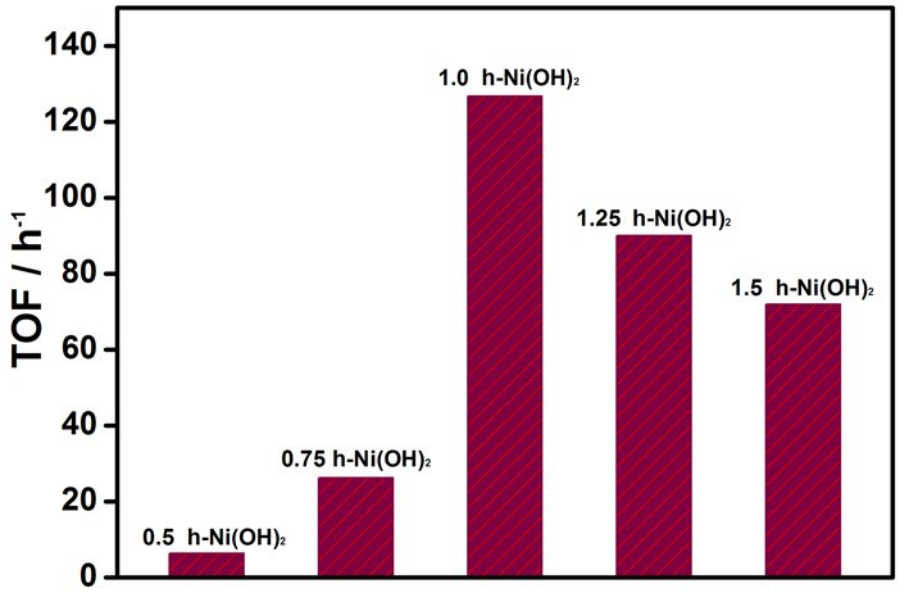

Figure S17. TOF of 0.5, 0.75, 1.0, 1.25 and 1.5 h-Ni(OH)$_2$.

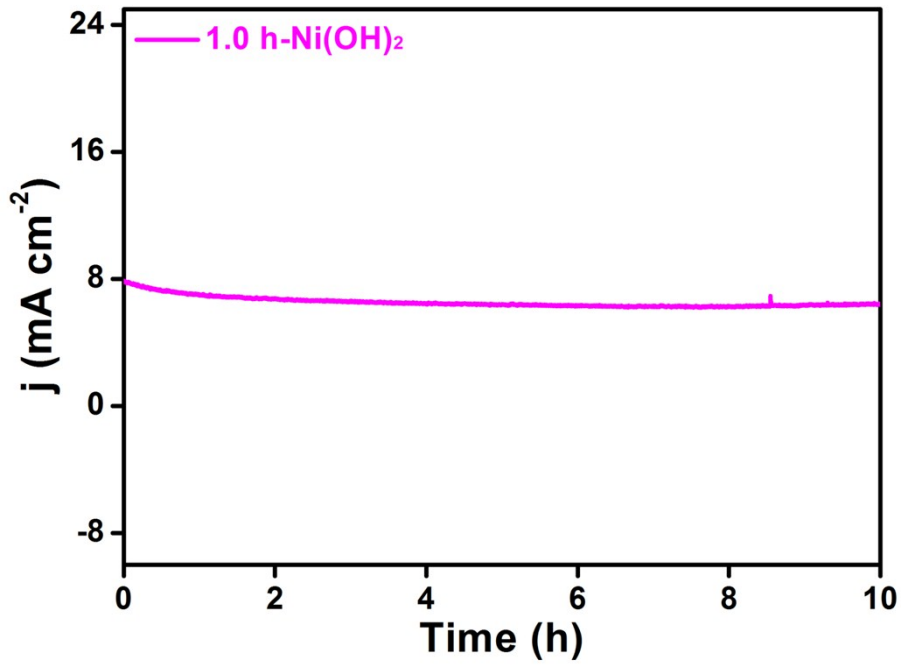

Figure S18. Durability test of 1.0 h-Ni(OH)$_2$ at 1.42 V versus RHE for electrolytic water oxidation .

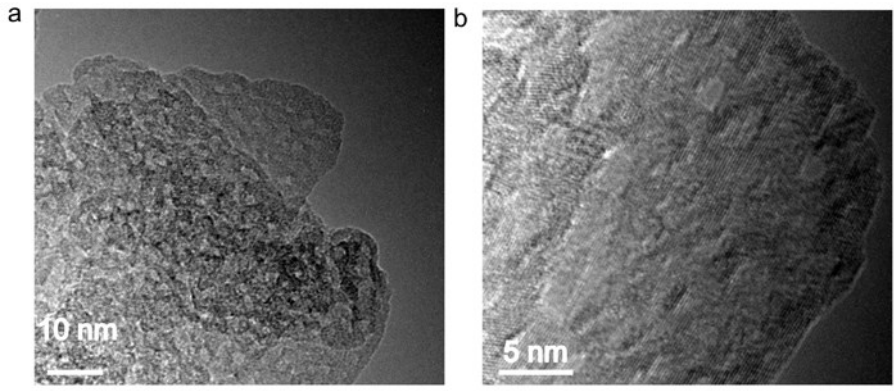

Figure S19. TEM images of 1.0 h-$Ni(OH)_2$ after durability test.

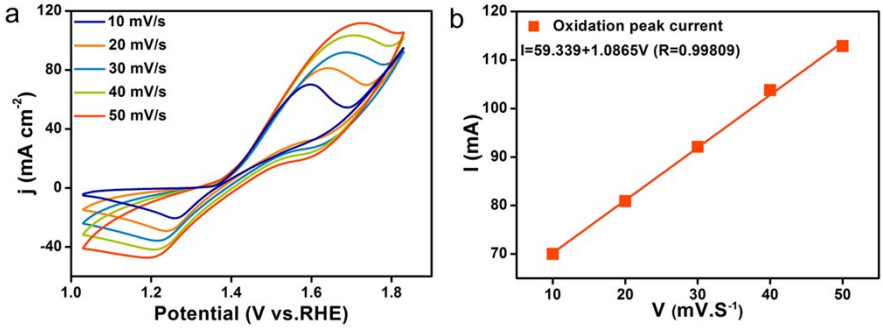

Figure S20. (a) The cyclic voltammograms of benzyl alcohol at various scan rates on 1.0 h-$Ni(OH)_2$. (b) I-V relationship of 1.0 h-$Ni(OH)_2$ from (a) in alkaline solution.

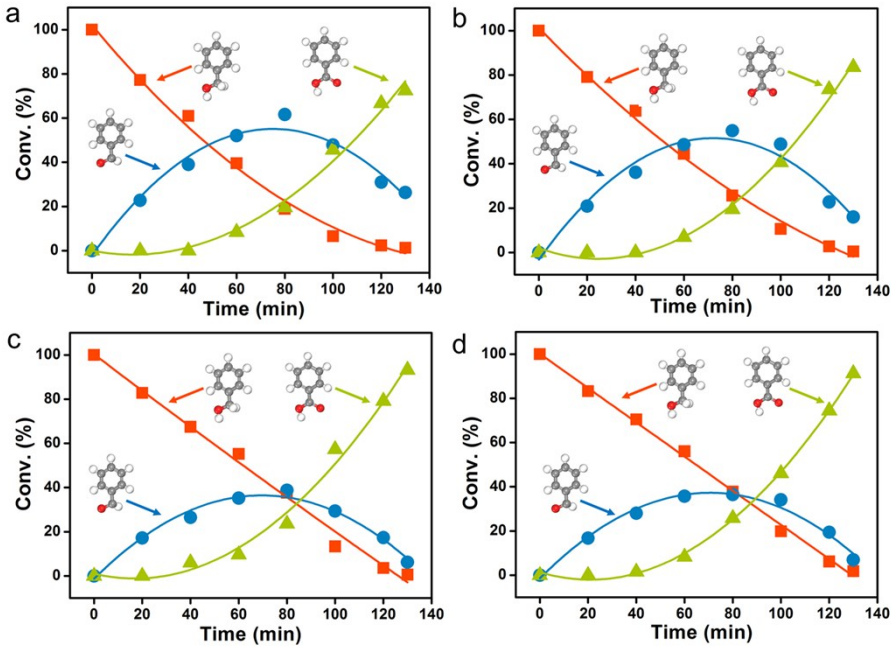

Figure S21. Conversion (%) of benzyl alcohol and selectivity (%) of oxidation products during the electrooxidation at a constant current of 20 mA in 1.0 m KOH with 40 × 10^{-3} M benzyl alcohol on (a) 0.5 h-Ni(OH)$_2$, (b) 0.75 h-Ni(OH)$_2$, (c) 1.25 h-Ni(OH)$_2$, (d) 1.5 h-Ni(OH)$_2$.

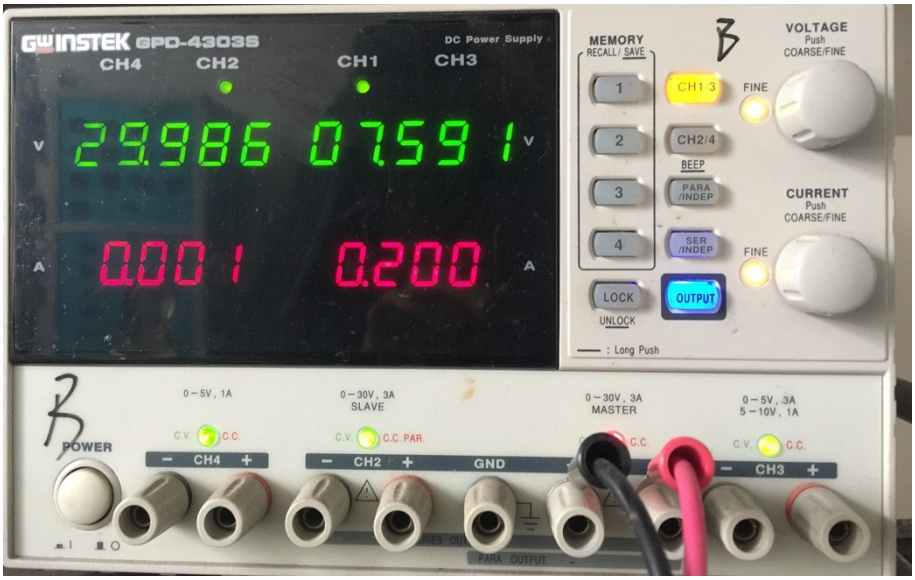

Figure S22. The photograph of constant current meter with concentration of 40 × 10^{-2} M benzoyl alcohol in ECO reaction.

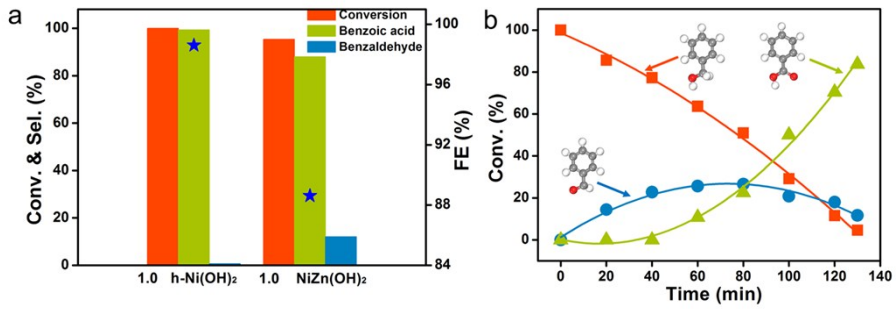

Figure S23. (a) Conversion of benzyl alcohol and selectivity to benzoic acid and benzaldehyde and faradaic efficiency in 1.0 h-Ni $(OH)_2$ and 1.0 $NiZn(OH)_2$. (b) Conversion (%) of benzyl alcohol and selectivity (%) of oxidation products on 1.0 $NiZn(OH)_2$.

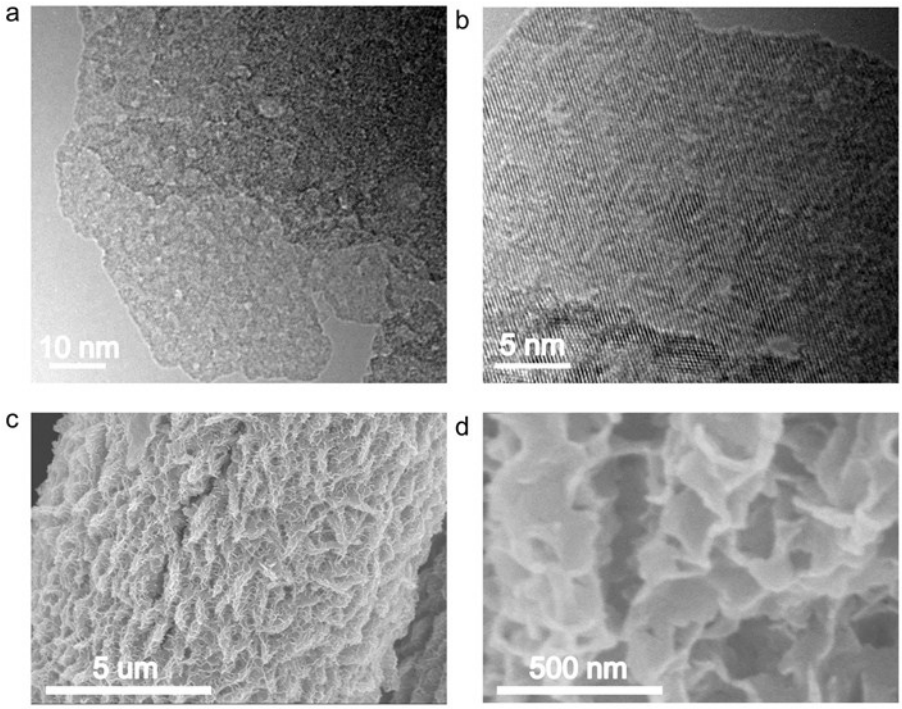

Figure S24. (a, b) TEM images and (c, d) SEM images of 1.0 h-$Ni(OH)_2$ after recycling measurement.

Table S3. Comparison of 1.0 h-$Ni(OH)_2$ and other electrocatalysts on ECO of benzyl alcohol to benzoic acid.

Catalyst	Main product	Conv（%）	Sel（%）	FE（%）	Reference
1.0 h-$Ni(OH)_2$	Benzoic acid	99.9	99.3	98.6	This work
Ni foam	Benzoic acid	93.69	75.85	81.52	This work
Co_3O_4 NWs/Ti	Benzoic acid	99	92	56.82	ACS Nano, 2017, 11, 12365-12377
$Co_{0.83}Ni_{0.17}$ /AC	Benzoic acid	100	99.4	96	New J. Chem., 2018, 42, 6381

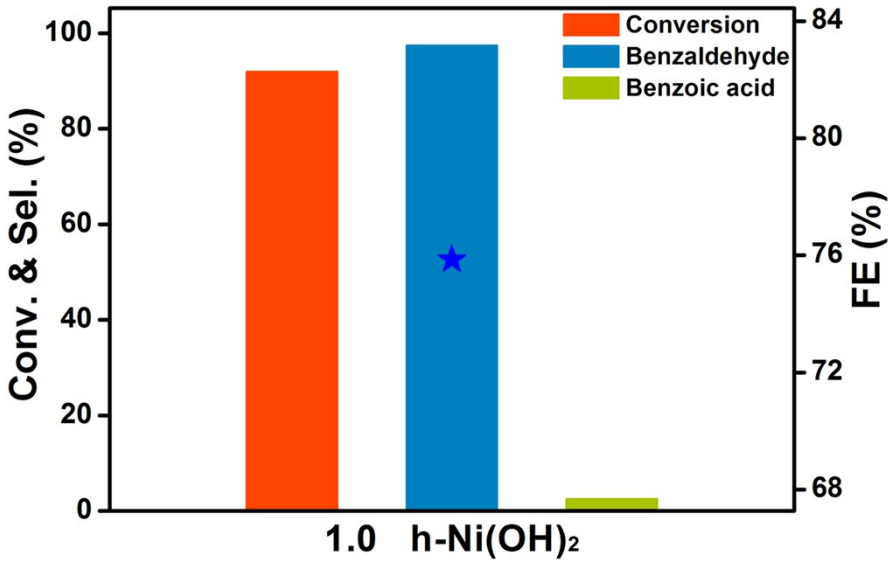

Figure S25. Conversion of benzyl alcohol and selectivity to benzoic acid and benzaldehyde and Faradaic efficiency in 1.0 h-$Ni(OH)_2$ after introducing TEMPO. Pentagonal stars represent Faraday efficiency.

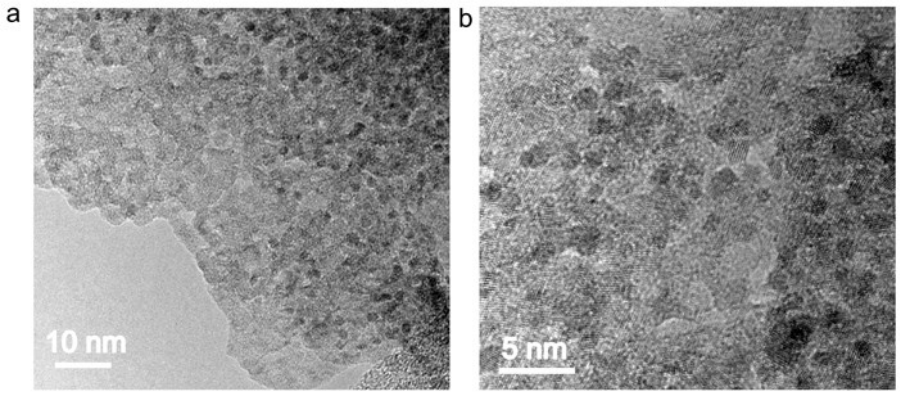

Figure S26. TEM images of 1.0 PtO_2/h-$Ni(OH)_2$.

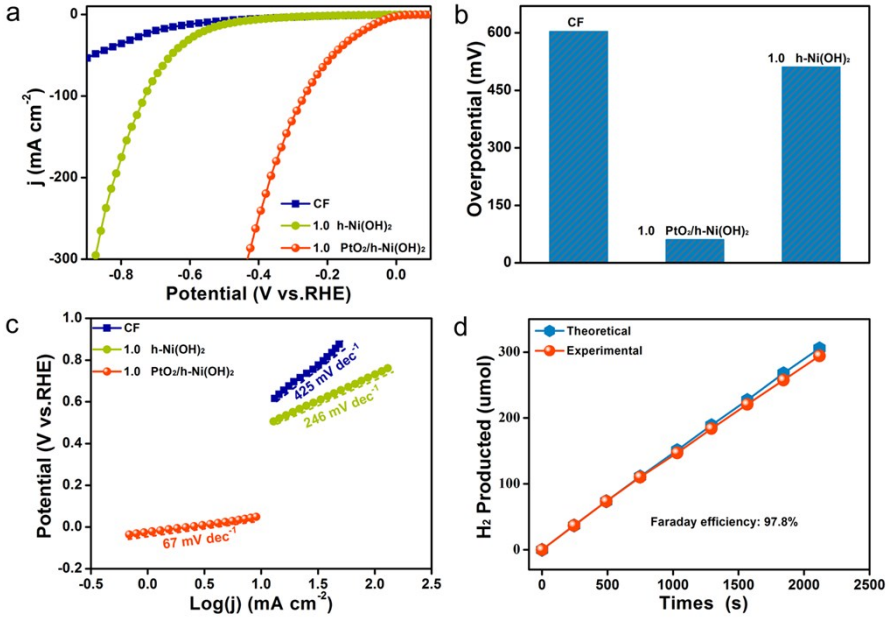

Figure S27. (a) HER polarization curves of the 1.0 PtO_2/h-$Ni(OH)_2$, 1.0 h-$Ni(OH)_2$ and CF. (b) Overpotential required at 10mA cm^{-2}. (c) Tafel plots derived from LSV curves of CF, 1.0 h-$Ni(OH)_2$ and 1.0 PtO_2/h-Ni $(OH)_2$. (d) The HER Faradaic efficiency of the 1.0 PtO_2/h-$Ni(OH)_2$ catalyst in 1.0 M KOH.

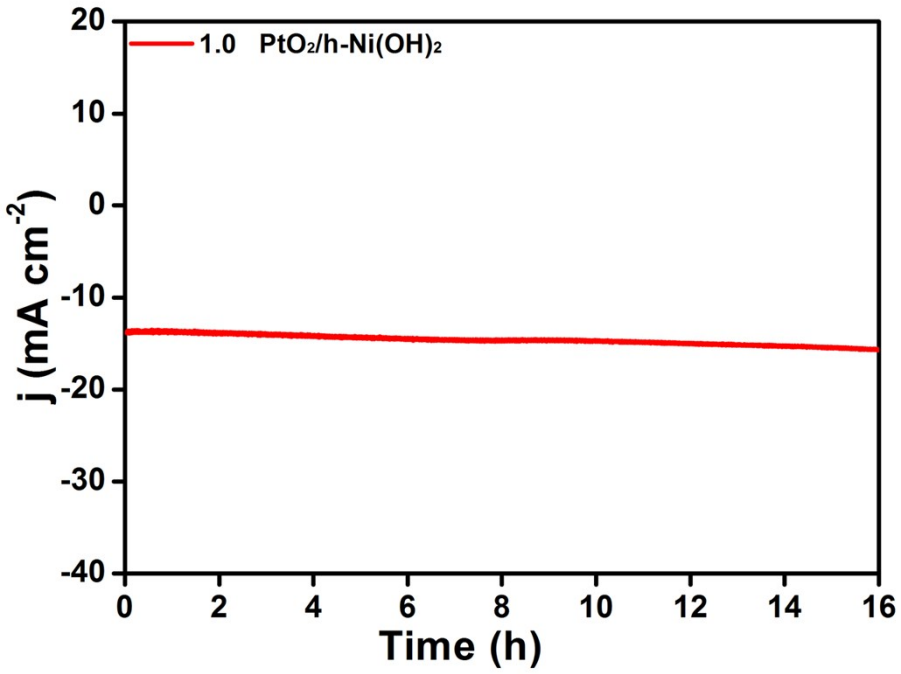

Figure S28. Chronopotentiometry curve of 1.0 PtO_2/h-$Ni(OH)_2$ at -0.076 V versus RHE.

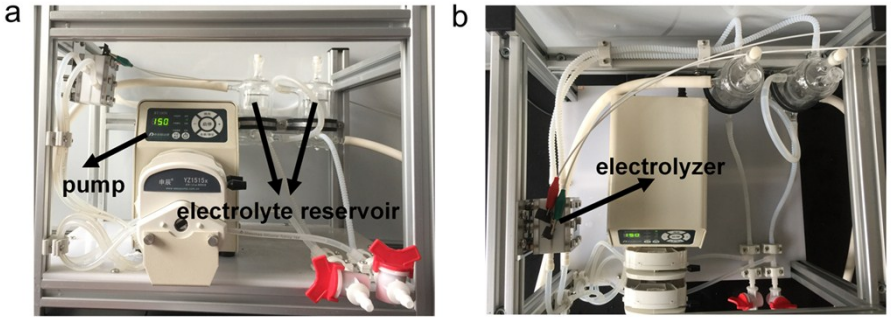

Figure S29. (a, b) The photograph of paired electrolysis system.

Table S4. The charge numbers of benzyl alcohol and oxygen atom in benzyl alcohol on vacancy-free $Ni(OH)_2$ and V_O-$Ni(OH)_2$.

Models	**oxygen atom in benzyl alcohol**	**benzyl alcohol**
vacancy-free $Ni(OH)_2$	-1.151	-0.047
V_O-$Ni(OH)_2$	-1.260	-0.114